Ashdin Publishing
Bioceramics Development and Applications
Vol. 1 (2011), Article ID D110128, 4 pages
doi:10.4303/bda/D110128

Research Article

Effect of Particle Size of Magnetite Nanoparticles on Heat Generating Ability under Alternating Magnetic Field

Z. Li,[1] M. Kawashita,[1] N. Araki,[2] M. Mistumori,[3] and M. Hiraoka[3]

[1] *Department of Biomedical Engineering, Graduate School of Biomedical Engineering, Tohoku University, Sendai, Miyagi 980-8579, Japan*
[2] *Department of Radiology, National Hospital Organization, Kyoto Medical Center, Kyoto 612-8555, Japan*
[3] *Department of Radiation Oncology and Image-Applied Therapy, Graduate School of Medicine, Kyoto University, Kyoto 606-8507, Japan*
Address correspondence to M. Kawashita, m-kawa@ecei.tohoku.ac.jp

Received 11 November 2010; Accepted 2 December 2010

Abstract In this study, magnetite nanoparticles (MNPs) with series of size varying from 8 nm to 103 nm were synthesized by a chemical co-precipitation and an oxidation-precipitation method to aim for finding the optimum particle size which has high heating efficiency in the applied magnetic field (9.6–23.9 $kA \cdot m^{-1}$, 100 kHz). Their in vitro heating efficiencies in agar phantom, at a MNPs concentration of 58 mg $Fe \cdot ml^{-1}$, were measured in the applied field. The temperature increase (ΔT) of the agar phantom at 30 s was 9.3 °C for MNPs of 8 nm, exhibiting a high heating efficiency in a field intensity of 9.6 $kA \cdot m^{-1}$. The ΔT of agar was 55 °C for MNPs of 24 nm and 25 °C for MNPs of 8 nm in a field intensity of 23.9 $kA \cdot m^{-1}$. The excellent heating efficiency for MNPs of 24 nm might be a combined effect of relaxation loss and hysteresis loss of the magnetic particles.

Keywords magnetite nanoparticles; particle size; hysteresis loss; relaxation loss; hyperthermia

1 Introduction

Recently, the magnetic fluid hyperthermia as a safe method for cancer therapy has attracted a significant attention, which can increase the temperature in tumors to around 43 °C and therefore kill tumor cells with minimum damage to the normal tissue [1]. This method involves the introduction of ferromagnetic or superparamagnetic particles into the tumor tissue and then irradiation with an alternating current (AC) magnetic field. In general, magnetic particles generate heat under an external AC magnetic field by several physical mechanisms: relax loss or hysteresis loss, which strongly depends on the frequency of the external field as well as the nature of the particles such as particle size and surface modification. Ferromagnetic particles generate heat due to hysteresis loss and/or relaxation loss.

Recent researches mainly focused on the heating properties of superparamagnetic particles (6–15 nm in size) in AC magnetic field because of their good dispersibility. But it was difficult to let these small nanoparticles stay at the affected area for a long-term and repeated therapy. Therefore, ferromagnetic nanoparticles with larger size were inferred to be useful especially in tumors located deep inside the body. Little attention, however, has been paid to the heating properties of a ferromagnetic magnetic particle due to the fact that high magnetic field intensity larger than the coercive force (H_c) of particle is needed to induce hysteresis loss of magnetic particles. In this study, we attempted to prepare series of magnetite nanoparticles (MNPs) ranged from 8 nm to 103 nm in an aqueous solution and their in vitro heating properties were measured under the developed AC magnetic field. It is expected that such findings are useful for designing novel thermo seeds for hyperthermia.

2 Materials and methods

Sodium hydroxide (NaOH), iron (II) chloride ($FeCl_2$) and iron (III) chloride ($FeCl_3$) were dissolved in deionized and deoxygenated water. MNPs with different diameters were prepared by two chemical methods. Sample A was prepared in a co-precipitation method in order to obtain smaller MNPs. Namely, 37.5 mL of 0.1 M-$FeCl_2$ aqueous solution was mixed with 50 mL of 0.1 M-$FeCl_3$ aqueous solution, and then the mixed liquid was added into 935 mL of 21 mM-NaOH solution under stirring, followed by ultrasonic treatment for 20 min and finally aged at 36.5 °C for 8 h. Resultant precipitates were washed with pure water and ethanol, and then dried at 60 °C for 12 h under nitrogen (N_2) atmosphere. In addition, samples B, C, D and E were prepared using an oxidation-precipitation method in an $FeCl_2$-$NaNO_3$-NaOH aqueous system as described elsewhere [4]. The particle size was controlled by adjusting the concentrations of the reactants as well as the order in which reactants are added. The resultant MNPs were dried at 60 °C under N_2 atmospheres.

The crystalline phase of samples is measured by powder X-ray diffractometer (XRD). The morphology and size of samples were observed by transmission electron microscopy (TEM). The magnetic properties of samples were measured by vibrating sample magnetometer. The glass tubes with agar phantom in which samples were dispersed at 58 mg $Fe \cdot ml^{-1}$ were placed in an alternating magnetic field (9.6 or 23.9 $kA \cdot m^{-1}$, 100 kHz) and the heat generation of samples was studied by measuring the temperature rise in agar phantom with a fluoroptic thermometer.

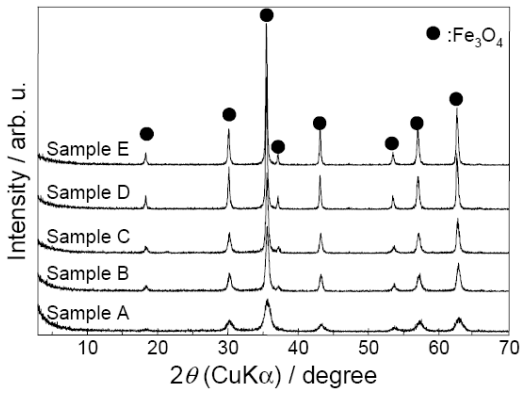

Figure 1: XRD patterns of samples.

3 Results and discussion

Figure 1 shows the XRD patterns of all samples that were formed in the solution by the co-precipitation method and oxidation-precipitation method. The XRD patterns were similar and consisted of sharp peaks which proved that all the synthesized nanoparticles can be identified as magnetite (Fe_3O_4) [2]. The lattice constant, a, calculated from the XRD patterns was 0.8393 nm for sample A, 0.8375 nm for sample B, 0.8371 nm for sample C, 0.8398 nm for sample D and 0.8388 for sample E. The lattice constants of all samples are closer to that of Fe_3O_4 (0.8396 nm) when compared to that of maghemite (γ-Fe_2O_3) (0.8345 nm) [6]. These indicate that samples were mainly composed of Fe_3O_4 phase with a small amount of γ-Fe_2O_3.

Figure 2 shows the TEM photographs of all samples. Samples A, B and C contained nearly spherical particles, samples D and E were composed of square-shaped with a little of spherical particles. Figure 2 also shows that the agglomeration of particles occurred in all samples, which is due to the magnetic interaction between the nanoparticles. The particle sizes for samples A, B, C, D and E estimated by TEM were around 8, 24, 36, 65 and 103 nm, respectively.

The saturation magnetization (M_s) and coercive force (H_c) of samples are presented in Table 1. The decreased M_s for samples A, B and C are attributed to the disordered surface spins and/or partially the existence of γ-Fe_2O_3 in these samples because γ-Fe_2O_3 has a lower M_s (56 $Am^2 \cdot kg^{-1}$) than Fe_3O_4 (92 $Am^2 \cdot kg^{-1}$) [3]. Particles in sample A are superparamagnetic with no coercivity and remanence. Particles in sample B, C and D are single domain, (H_c) increased with increasing particles size until 65 nm (sample D). Particles in sample E (103 nm in size) are inferred to be multidomain [5].

The heat generation (P) caused by the hysteresis loss of samples at given alternating magnetic field can be estimated by integrating the measured hysteresis loop area. The estimated heat generation at 23.9 $kA \cdot m^{-1}$, 100 kHz is given in Table 1. For sample A, hysteresis loss contribution was extremely little due to their superparamagnetic properties. Sample B (24 nm in size) exhibited the largest loop area (data were not shown), indicating the best heating efficiency in the AC magnetic field.

Figure 3 shows the time-dependent temperature curves of agar phantoms, in which samples were dispersed, in two different AC magnetic fields: (a) 9.6 $kA \cdot m^{-1}$, 100 kHz and (b) 23.9 $kA \cdot m^{-1}$, 100 kHz. In the field intensity of 9.6 $kA \cdot m^{-1}$ (see Figure 3(a)), temperature increase (ΔT) of the agar phantom at 30 s was 9.3 °C for sample A, 2 °C for sample B and around 1 °C for the others. Due to superparamagnetic properties, relaxation loss mainly contributes to heat generation of samples A. In addition, the applied external magnetic field intensity (9.6 $kA \cdot m^{-1}$) was much lower than the H_c of samples C, D and E (see Table 1), and hence the heat generations due to hysteresis loss became unavailable for these samples.

In the magnetic field of 23.9 $kA \cdot m^{-1}$ (see Figure 3(b)), ΔT in agar phantom at 30 s was 55 °C for sample B, 25 °C for sample A, and decreased with increasing particle size (i.e. B > C > D > E). Sample B exhibited a high heating efficiency in the AC magnetic field. The tendency of heat generation to vary with the particles size was matched with the tendency of hysteresis loop area (data were not shown). In this case, the applied external magnetic field strength (23.9 $kA \cdot m^{-1}$) was much higher than the H_c of all samples, hence the heat generations were derived mainly from hysteresis loss of these samples in AC magnetic field. As can be seen in Figure 2, Sample B also contained

Sample	M_s/$Am^2 \cdot kg^{-1}$	H_c/$kA \cdot m^{-1}$	P/$W \cdot g^{-1}$
A	67.3	0.7	0.33
B	76.5	8.4	16.5
C	76.7	11.1	8.1
D	89.2	15.1	6.6
E	79.3	13.9	4.9

Table 1: Saturation magnetization (M_s) and coercive force (H_c) of samples and estimated heat generation (P) which is caused by hysteresis loss of samples under an alternating magnetic field of 23.9 $kA \cdot m^{-1}$, 100 kHz.

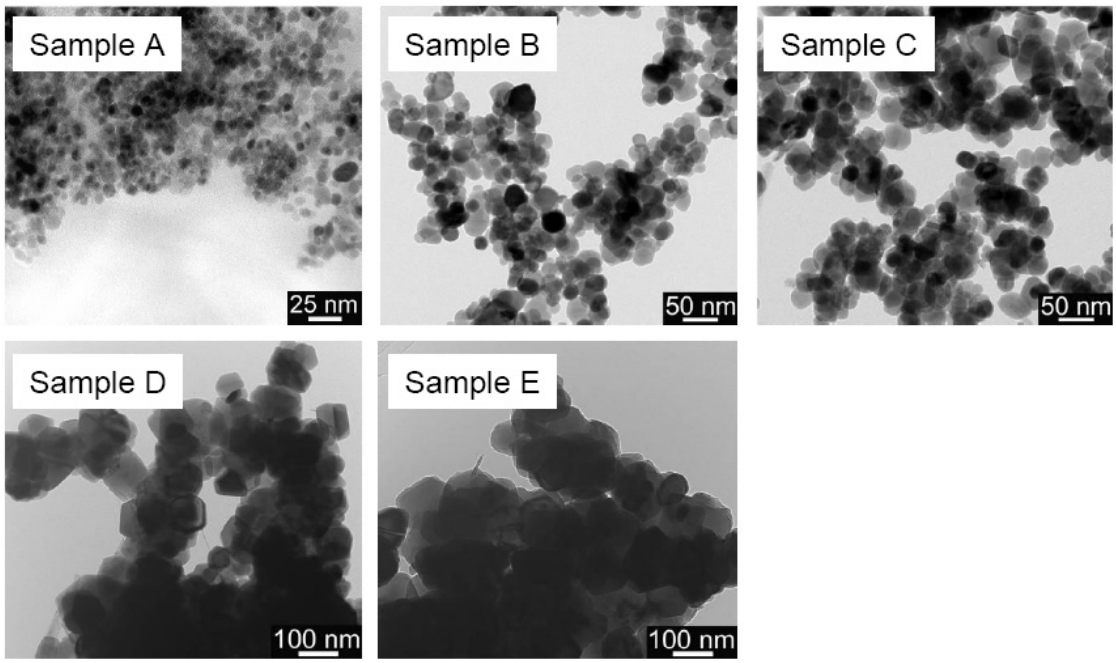

Figure 2: TEM photographs of samples.

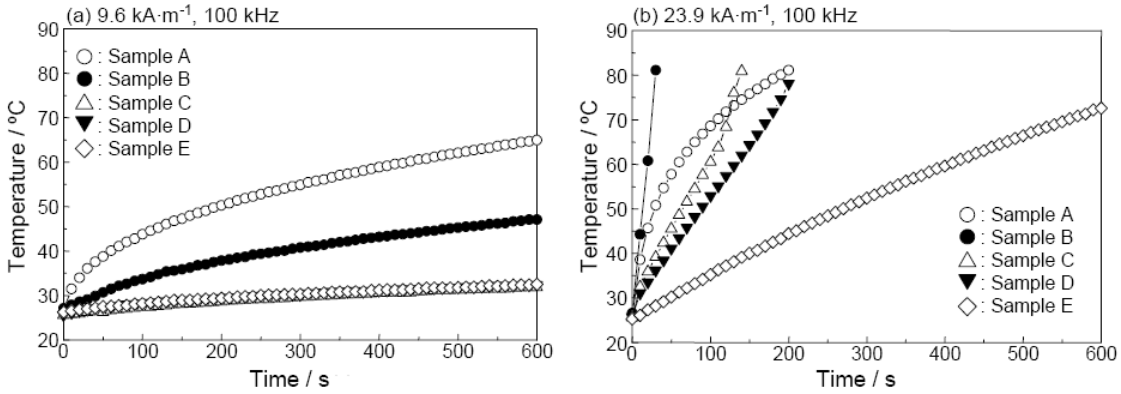

Figure 3: Time-dependent temperature curves of agar phantoms, in which samples were dispersed, in two different AC magnetic fields: (a) 9.6 kA·m^{-1}, 100 kHz and (b) 23.9 kA·m^{-1}, 100 kHz.

some smaller superparamagnetic particles ($<$ 20 nm), thus relaxation loss contributed to partial heat generation of sample B.

4 Conclusions

Magnetite nanoparticles with different sizes were prepared using a chemical co-precipitation method and oxidation-precipitation method, and their magnetic properties and heat generations in an external alternating magnetic field were investigated. The particles 8 nm in diameter exhibited a high heating efficiency in an alternating magnetic field of 9.6 kA·m^{-1}, 100 kHz, and the heating efficiency of the particles was improved with decreasing particle size from 103 nm to 24 nm in the alternating magnetic field of 23.9 kA·m^{-1}, 100 kHz. The results suggest that the heat generation is not simply a question of particle size but also is highly dependent on magnetic field intensity. The heating efficiency was best in the particles 24 nm in diameter in the applied magnetic field of 100 kHz and 23.9 kA·m^{-1}, which might be a combined effect of relaxation loss and hysteresis loss of the magnetic particles.

Acknowledgments This work was partially supported by Funds for Promoting Science and Technology under the Program for Exploring Advanced Interdisciplinary Frontiers, the Ministry of Education, Culture, Sports, Science and Technology, Japan, and Research Grants from the Kazuchika Okura Memorial Foundation, Japan.

References

[1] A. Ito and T. Kobayashi, *Intracellular hyperthermia using magnetic nanoparticles: a novel method for hyperthermia clinical applications*, Thermal Med, 24 (2008), pp. 113–129.

[2] G. W. Leung, M. E. Vickers, R. Yu, and M. G. Blamire, *Epitaxial growth of Fe_3O_4 (1 1 1) on $SrTiO_3$ (0 0 1) substrates*, J Cryst Growth, 310 (2008), pp. 5282–5286.

[3] B. Li, D. Jia, Y. Zhou, Q. Hu, and W. Cai, *In situ hybridization to chitosan/magnetite nanocomposite induced by the magnetic field*, J Magn Magn Mater, 306 (2006), pp. 223–227.

[4] Z. Li, M. Kawashita, N. Araki, M. Mitsumori, and M. Hiraoka, *Preparation of size-controlled magnetite nanoparticles for hyperthermia of cancer*, Trans MRS-J, 34 (2009), pp. 77–80.

[5] M. Ma, Y. Wu, J. Zhou, Y. Sun, Y. Zhang, and N. Gu, *Size dependence of specific power absorption of Fe_3O_4 particles in ac magnetic field*, J Magn Magn Mater, 268 (2004), pp. 33–39.

[6] T. Ozkaya, M. S. Toprak, A. Baykal, H. Kavas, Y. Koseoglu, and B. Aktas, *Synthesis of Fe_3O_4 nanoparticles at 100 °C and its magnetic characterization*, J Alloy Compd, 472 (2009), pp. 18–23.